


openheart Non-invasive intraventricular pressure differences estimated with cardiac MRI in subjects without heart failure and with heart failure with reduced and preserved ejection fraction

Francisco Londono-Hoyos,^{1,2} Patrick Segers,² Zeba Hashmath,¹ Garrett Oldland,^{1,3} Maheshwara Reddy Koppula,¹ Khuzaima Javid,³ Rachana Miller,^{1,3} Rushikkumar Bhuvu,^{1,3} Izzah Vasim,^{1,3} Ali Tariq,³ Walter Witschey,¹ Scott Akers,³ Julio Alonso Chirinos ^{1,2,3}

To cite: Londono-Hoyos F, Segers P, Hashmath Z, *et al*. Non-invasive intraventricular pressure differences estimated with cardiac MRI in subjects without heart failure and with heart failure with reduced and preserved ejection fraction. *Open Heart* 2019;**6**:e001088. doi:10.1136/openhrt-2019-001088

Received 13 May 2019
Revised 24 June 2019
Accepted 11 September 2019



© Author(s) (or their employer(s)) 2019. Re-use permitted under CC BY-NC. No commercial re-use. See rights and permissions. Published by BMJ.

¹Hospital of the University of Pennsylvania and University of Pennsylvania, Philadelphia, Pennsylvania, USA

²Institute Biomedical Technology (IBiTech) - bioMMeda Research Group, Ghent University, Ghent, Belgium

³Corporal Michael J. Crescenz VAMC, Philadelphia, Pennsylvania, USA

Correspondence to

Dr Julio Alonso Chirinos; julio.chirinos@uphs.upenn.edu

ABSTRACT

Objective Non-invasive assessment of left ventricular (LV) diastolic and systolic function is important to better understand physiological abnormalities in heart failure (HF). The spatiotemporal pattern of LV blood flow velocities during systole and diastole can be used to estimate intraventricular pressure differences (IVPDs). We aimed to demonstrate the feasibility of an MRI-based method to calculate systolic and diastolic IVPDs in subjects without heart failure (No-HF), and with HF with reduced ejection fraction (HFrEF) and HF with preserved ejection fraction (HFpEF).

Methods We studied 159 subjects without HF, 47 subjects with HFrEF and 32 subjects with HFpEF. Diastolic and systolic intraventricular flow was measured using two-dimensional in-plane phase-contrast MRI. The Euler equation was solved to compute IVPDs in diastole (mitral base to apex) and systole (apex to LV outflow tract).

Results Subjects with HFpEF demonstrated a higher magnitude of the early diastolic reversal of IVPDs (−1.30 mm Hg) compared with the No-HF group (−0.78 mm Hg) and the HFrEF group (−0.75 mm Hg; analysis of variance $p=0.01$). These differences persisted after adjustment for clinical variables, Doppler-echocardiographic parameters of diastolic filling and measures of LV structure (No-HF=−0.72; HFrEF=−0.87; HFpEF=−1.52 mm Hg; $p=0.006$). No significant differences in systolic IVPDs were found in adjusted models. IVPD parameters demonstrated only weak correlations with standard Doppler-echocardiographic parameters.

Conclusions Our findings suggest distinct patterns of systolic and diastolic IVPDs in HFpEF and HFrEF, implying differences in the nature of diastolic dysfunction between the HF subtypes.

INTRODUCTION

The incidence and prevalence of heart failure (HF) is increasing worldwide.¹ Clinically, two major subtypes of HF are identified^{2–4} based on the left ventricular (LV) ejection

Key questions

What is already known about this subject?

► Both systolic and diastolic dysfunction are present in heart failure (HF) with reduced (HFrEF) and with preserved ejection fraction (HFpEF). Thus, a better understanding of the nature of physiological abnormalities in subjects with HF is essential to improve its management. Non-invasive quantitative analysis of intraventricular flow dynamics, such as blood flow velocities, provide important insights into the processes driving left ventricular (LV) ejection and filling. The spatiotemporal pattern of LV blood flow velocities can provide additional information from estimations of underlying intraventricular pressure differences (IVPDs) driving diastolic and systolic intraventricular flow in HFrEF and HFpEF.

What does this study add?

► Our study demonstrated the feasibility to assess IVPDs throughout the cardiac cycle using phase-contrast MRI and comparing IVPDs between subjects without HF and subjects with HFrEF and HFpEF. The proposed MRI-based method is more flexible in terms of the definition and alignment of the operator's 'scan line', and thus in the potential analysis conducted, than the echocardiographic standard approach and could be performed complementary to routine MRI protocols. Furthermore, our findings suggest distinct patterns of systolic and diastolic IVPDs in HFpEF and HFrEF, implying differences in the nature of diastolic dysfunction between the HF subtypes.

How might this impact on clinical practice?

► Further research is warranted to exploit MRI analysis thoroughly to assess the significance of these novel indices regarding risk stratification and response to therapy.

fraction (EF): HF with reduced (HFrEF) and with preserved EF (HFpEF).^{2–4} Although LV systolic dysfunction is thought to be the

key pathophysiological abnormality in HFrEF, diastolic dysfunction is also present in this condition. Similarly, whereas diastolic dysfunction is thought to be a key pathophysiological abnormality in HFpEF, systolic contractile abnormalities have been also reported in this condition. Therefore, a better understanding of the nature of physiological abnormalities in HF patients is desirable.

Non-invasive quantitative analysis of intraventricular flow dynamics can provide important insights into the processes driving LV ejection and filling. While the analysis of blood flow velocities (in particular, the transmitral flow velocities) is extensively used in the evaluation of LV function,^{5–7} much less is known about underlying pressure differences driving diastolic and systolic intraventricular flow in HFrEF and HFpEF. These pressure differences can be inferred by solving the Euler equation, a simplified version of the Navier-Stokes equations,^{8,9} using information regarding the spatiotemporal pattern of LV blood flow velocities, which in turn can be obtained using ultrasound (eg, colour M-mode recordings along a transmitral scanline) or MRI. The computation of intraventricular pressure differences (IVPDs) has been applied in the context of diastolic function analysis but can also be applied to systole, to interrogate pressure gradients produced by LV ejection.

The aim of this study is to demonstrate the feasibility of an MRI-based method to characterise IVPDs throughout diastole and systole.

METHODS

We prospectively enrolled a sample of patients at the Corporal Michael J. Crescenz VA Medical Center. The protocol was approved by the Philadelphia VA Medical Center Institutional Review Board, and all subjects provided written informed consent.

HFrEF was defined as a symptomatic HF in the presence of a left ventricular ejection fraction (LVEF) <50%. HFpEF was defined as the presence of all of the following: (1) New York Heart Association (NYHA) Class II–IV symptoms consistent with HF; (2) LV ejection fraction >50%; (3) Mitral inflow early diastolic (E wave) to annular tissue velocity (e') ratio >14,¹⁰ or at least two of the following: (a) an average mitral E/e' ratio >8; (b) treatment with a loop diuretic for control of HF symptoms; (c) left atrial volume index >34 mL/m² of body surface area; (d) NT-pro B-type natriuretic peptide level >200 pg/mL; (e) LV mass index >149 g/m² in men and 122 g/m² in women (measured by cardiac MRI).¹¹ No-HF subjects had an LVEF >50%, no significant valvular disease, and no symptoms and signs consistent with HF.¹²

Key exclusion criteria were: (1) claustrophobia; (2) presence of metallic objects or implanted medical devices in body; (3) more than mild aortic stenosis; (4) atrial fibrillation; (5) conditions that would make the study measurements less accurate or unreliable (ie, arrhythmia affecting cardiac gating, inability to perform an adequate breath hold for cardiac MRI acquisitions); (6) known

infiltrative or hypertrophic cardiomyopathy, or extracardiac amyloidosis or sarcoidosis.¹²

Doppler echocardiography

Doppler transthoracic echocardiography was performed at rest with the patient in supine position using a Vivid E9 device (GE Healthcare, Horten, Norway), equipped with a cardiac probe.

Two-dimensional phase contrast imaging acquisition and processing

Intraventricular flow velocities were measured with phase-contrast MRI, using a 1.5T MRI scanner (Avanto system; Siemens Healthcare; Erlangen, Germany). A phase contrast gradient echo pulse sequence with in-plane velocity encoding was applied using retrospective gating in a plane corresponding to the three-chamber view ('LV outflow tract view') in which both the mitral inflow and the LV outflow are well visualised. We performed two consecutive breath-held acquisitions, each with in-plane velocity encoding in one direction. Both acquisitions were merged offline to obtain the in-plane two-dimensional-velocity maps. Images were obtained with the following imaging parameters: TE=2.7 ms, TR=4.8 ms, temporal resolution=39.8 ms, bandwidth=450 Hz/pixel, field-of-view=360×360 mm², matrix=152–192×256, spatial resolution=1.88×1.88 mm², slice thickness=6 mm, flip angle=20°. Maximal velocity encoding was usually set at 130 cm/s but adjusted during the examination to avoid aliased velocity measurements.

Image processing and computation of IVPDs

A MATLAB (MathWorks, Natick, Massachusetts, USA) custom-designed graphic user interface was programmed to process all phase-contrast MRI sequences. The pressure difference between two points in a plane (the scanning plane) can be calculated from the two-dimensional planar velocity information as¹³

$$\text{IVPD} = \sum_i \left[\left(\frac{\partial P}{\partial x} \right)_i x_i + \left(\frac{\partial P}{\partial y} \right)_i y_i \right] \quad (1)$$

with pressure derivatives linked through the Euler equation to the two-dimensional-velocity information:

$$\frac{\partial P}{\partial x, y} = -\rho \left[\frac{\partial u_{x,y}}{\partial t} + u_x \frac{\partial u_{x,y}}{\partial x} + u_y \frac{\partial u_{x,y}}{\partial y} \right] \quad (2)$$

with u the two-dimensional-component vector (u_x, u_y) of local blood velocity and ρ , blood density (1060 Kg/m³).

The instantaneous pressure difference between any two points along this streamline ($\frac{\partial P}{\partial s}$), is the net result of the change in velocity with time at a given spatial point (*inertial* component, $\left(\frac{\partial u}{\partial t} \right)$), and the change in velocity with space at any given time (*convective* component, $\left(u \frac{\partial u}{\partial s} \right)$).⁸

For the assessment of diastolic IVPDs, 2–4 reference points were placed inside the LV along the inflow direction at the mitral annulus (Point 1, P1) and the LV apex (Point 2, P2) (figure 1A, B). For the assessment of systolic IVPDs, 2–4 reference points were placed along the outflow direction, from the LV apex (P1) to

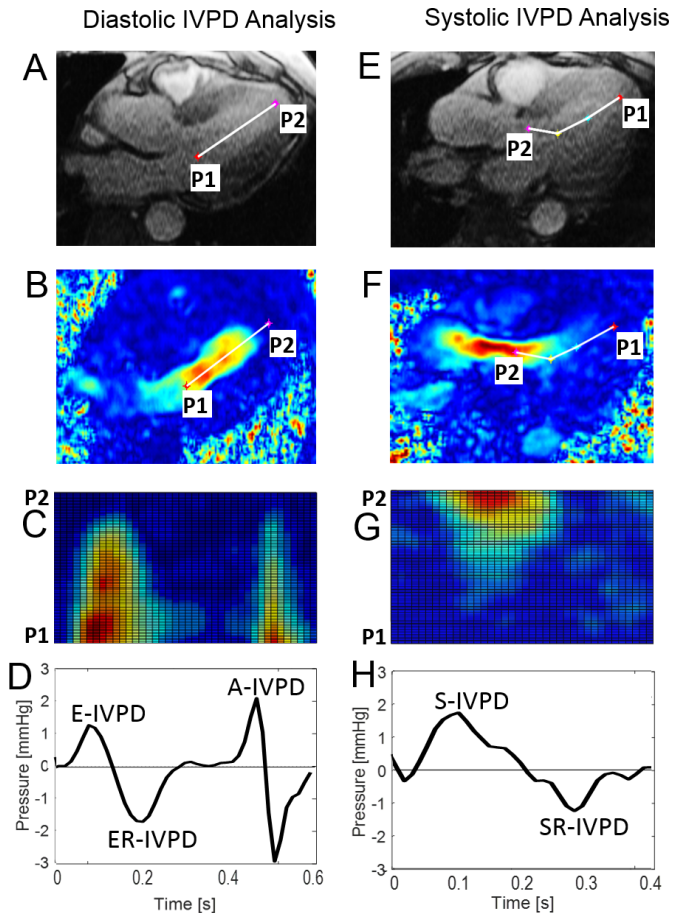


Figure 1 Graphical description of the phase-contrast MRI sequence processing to assess diastolic function (left column) and systolic function (right column). (A) and (E) original magnitude images and (B) and (F) calculated velocity vectors images, showing the reference points selection, located at: (left) the mitral annulus (P1) and LV apex (P2); and (right) LV apex (P1) and aortic annulus (P2). (C) and (G) the pseudo colour M-mode image, calculated from the two-dimensional velocity vectors, was used as quality reference of the IVPD curves. Calculated IVPD curves (solid black line): (D) during diastole, showing the (1) E-wave (E-IVPD), (2) reversal E-wave (ER-IVPD) and (3) A-wave (A-IVPD) pressure peaks, and (H) during systole, showing the (1) S-wave (S-IVPD) and (2) reversal S-wave (SR-IVPD) pressure peaks. (C, D) and (G, H) are aligned in time, respectively. Important to REMARK, the colour scale in (B, C, F) and (G) is a visual guidance for the user during the processing, and the linear (two points) and the curvilinear (four points) approximation could be selected by the user for diastolic and/or systolic analysis. IVPD, intraventricular pressure difference.

the aortic annulus (P2) (figure 1E, F). To note, points were: (1) placed using the frame with the best anatomical view of the structures and (2) stationary through the whole cardiac cycle. A pseudo-colour M-mode image was calculated projecting velocity components within the path delimited by the reference points and displayed for processing visual guidance (figure 1C, G).

Available velocity components were used to calculate pressure gradient fields and differences. Then, interpolated values along the line delimited by P1 and P2 were

used to solve equation 1, applying a direct integration method¹³ to obtain the IVPD curves (figure 1D, H).

Statistical analysis

Descriptive data are presented as mean \pm SD or mean (95% CI) for continuous variables or counts (%) for categorical variables. Differences between groups were determined by one-way analysis of variance (ANOVA) and adjusted for potential confounders. Physiological indices were expressed as absolute values as well as absolute differences between measurements (with 95% CIs). A p value <0.05 was considered statistically significant. We presented a model with unadjusted data, and three adjusted models: model 1—adjusted for clinical data (age, sex, African American ethnicity, body mass index (BMI), coronary artery disease, estimated glomerular filtration rate (eGFR) and beta-blocker, ACE-Inhibitor/angiotensin receptor blocker (ARB), loop diuretic and spironolactone use); model 2—model 1 additionally adjusted for echo parameters (Mitral E-wave velocity, E-wave deceleration time, Mitral annular e' septal); model 3—model 2 additionally adjusted for MRI data (LV mass index and end-diastolic volume index (EDVI)). Statistical analyses were performed using MATLAB statistics and machine learning toolbox (Matlab 2016b, the Mathworks; Natwick, Massachusetts, USA) and SPSS for Mac V.22.

Reproducibility and repeatability assessment

To test the method's reproducibility (measurements performed by two different operators at least 1 year apart) and repeatability (measurements performed by the same operator at least 1 week apart), 10 cases (included in the study) were assessed, calculating the Pearson r-value squared (r^2), the sum of squared error (SSE) and the reproducibility coefficient (RPC).

Echocardiographic/MRI correlation assessment

To evaluate the potential added value of the proposed technique, correlation coefficients were calculated between selected MRI parameters and established Doppler-echocardiographic indices of diastolic function.

RESULTS

General characteristics of the study population are shown in table 1. The mean age of participants with HFrEF, HFpEF and without HF was 65.9, 62.9 and 61.8 years, respectively. The HFrEF group demonstrated a high prevalence of hypertension, diabetes, coronary artery disease and pronounced left atrial enlargement. Consistent with the HFpEF phenotype, subjects in this group were obese and had a high prevalence of hypertension and diabetes. Most subjects with HFrEF and HFpEF were receiving beta blockers, an ACE inhibitor or ARB, and loop diuretics. The study sample was composed predominantly of males, with a high proportion of African-Americans, particularly in the HFrEF group.

Table 1 General characteristics of study subjects

Variable	No-HF (n=159)	HFrEF (n=47)	HFpEF (n=32)	P value
Age (years)	61.8±11.5	65.9±10.7	62.9±8.6	0.09
Male	145 (91)	46 (98)	28 (88)	0.18
Race				
African-American	72 (45)	31 (66)	16 (50)	0.04*
Caucasian	74 (47)	15 (32)	15 (47)	0.20
BMI (kg/m ²)	29.5 (25.7, 33.1)	27.9 (24.2, 32.9)	35 (29.3, 41.7)	0.0007†‡
Heart rate (bpm)	68.9±13	69±11.9	67.4±11.9	0.84
Ejection duration (ms)	319±30	311±47	325±33	0.27
Current smoker	43 (28)	15 (33)	8 (25)	0.73
Hypertension	118 (75)	41 (89)	29 (91)	0.03
Diabetes	64 (41)	27 (59)	18 (56)	0.04*
Coronary artery disease	47 (30)	24 (51)	11 (34)	0.03*
Drug therapy				
Beta blocker	74 (47)	43 (91)	24 (75)	<0.0001*†
ACE-inhibitor/ARB	80 (51)	37 (79)	26 (81)	<0.0001*†
Calcium-channel blocker	41 (26)	12 (26)	13 (41)	0.23
Spironolactone	3 (2)	6 (13)	4 (13)	0.002*†
Statin	103 (65)	36 (77)	21 (66)	0.33
Aspirin	84 (53)	37 (79)	19 (59)	0.007*
Thiazide	34 (22)	11 (23)	5 (16)	0.74
Loop diuretics	2 (1)	35 (74)	23 (72)	<0.0001*†
eGFR (mL/min/1.73 m ²)§	86 (65, 99.8)	74 (56.5, 92.3)	84 (63, 99)	0.056*
LV EF (%)	59.6 (52.2, 65.6)	36.6 (23.7, 42.5)	61.4 (58, 70.3)	<0.0001*‡
LA volume index (mL/m ²)	30.7 (23.8, 39.5)	46.1 (35.7, 65.3)	36.6 (26.4, 49.9)	<0.0001*
LV EDVI (mL/m ²)	69.9 (58.4, 82.4)	102.7 (85.8, 141.4)	69.1 (56.7, 79.5)	<0.0001*‡
LV mass index BSA (g/m ²)	64.5 (56.9, 76.5)	88.6 (77.9, 107.1)	72 (59.3, 83.2)	<0.0001*‡
Mitral E-wave velocity (cm/s)	69.5 (58.1, 85.5)	74.3 (54.7, 93.6)	69.6 (60.5, 92.7)	0.54
Mitral E-wave deceleration time (ms)	210 (170, 240)	180 (140, 220)	220 (170, 270)	0.06
Mitral A-wave velocity (cm/s)	74.6±21.7	62.3±22.3	74.7±19.6	0.008*
Mitral annular e', septal (cm/s)	7.58 (5.9, 9.65)	5.61 (4.12, 7.9)	6.77 (5.24, 8.19)	0.0007*

Values are mean±SD or mean (95% CI), or counts (percentages).

*p<0.05 for No-HF vs HFrEF.

†p<0.05 for No-HF vs HFpEF.

‡p<0.05 for HFrEF vs HFpEF.

§eGFR was calculated using the Modification of Diet in Renal Disease Study equation.

ACE, angiotensin convertase enzyme; ARB, angiotensin receptor blocker; BSA, body surface area; EF, ejection fraction; eGFR, estimated glomerular filtration rate; HFpEF, HF with preserved ejection fraction; HFrEF, HF with reduced ejection fraction; LV, left ventricular.

In all three groups (No-HF, HFrEF and HFpEF), subjects exhibited, in general, consistent IVPD patterns described previously using colour M-mode Doppler echocardiography¹⁴⁻¹⁷ or cardiac MRI^{13 18 19} (figure 1D, H). The diastolic period of the calculated IVPD waveforms was typically characterised by (1) a large early diastolic forward positive difference (E-IVPD) during ventricular relaxation, associated with early diastolic rapid filling; (2) an early diastolic negative peak associated with the deceleration of the early filling (ER-IVPD); (3) a second, late diastolic, positive peak

(A-IVPD) associated with atrial contraction (see figure 1D). The systolic period was characterised by a typical biphasic configuration with (1) a large forward positive peak (S-IVPD) associated with ventricular systole (rapid ejection) followed by (2) a negative peak (SR-IVPD) associated with its deceleration (slow ejection phase) (see figure 1H). Selected IVPD parameters are shown and compared in table 2, and figures 2 and 3.

Table 2 Comparison of diastolic and systolic intraventricular pressure difference parameters between the groups

Variable	No-HF (n=159)	HFrEF (n=47)	HFpEF (n=32)	P value
Unadjusted model				
E-IVPD (mm Hg)	0.76 (0.68, 0.84)	0.83 (0.67, 0.98)	0.83 (0.64, 1.02)	0.63
ER-IVPD (mm Hg)	-0.78 (-0.93, -0.63)	-0.75 (-1.02, -0.47)	-1.30 (-1.60, -0.99)	0.01*†
A-IVPD (mm Hg)	0.93 (0.85, 1.02)	0.72 (0.56, 0.88)	0.92 (0.73, 1.11)	0.07
S-IVPD (mm Hg)	1.7 (1.56, 1.84)	1.41 (1.16, 1.65)	1.99 (1.65, 2.34)	0.01†
SR-IVPD (mm Hg)	-1.15 (-1.28, -1.02)	-0.90 (-1.17, -0.64)	-1.37 (-1.64, -1.10)	0.04†
Adjusted model 1				
E-IVPD (mm Hg)	0.75 (0.65, 0.85)	0.86 (0.64, 1.08)	0.85 (0.61, 1.08)	0.70
ER-IVPD (mm Hg)	-0.76 (-0.95, -0.56)	-0.85 (-1.23, -0.47)	-1.35 (-1.72, -0.97)	0.02*
A-IVPD (mm Hg)	0.94 (0.83, 1.05)	0.71 (0.49, 0.92)	0.94 (0.70, 1.17)	0.15
S-IVPD (mm Hg)	1.7 (1.52, 1.89)	1.49 (1.14, 1.84)	1.89 (1.47, 2.3)	0.16
SR-IVPD (mm Hg)	-1.15 (-1.32, -0.98)	-0.94 (-1.30, -0.58)	-1.34 (-1.67, -1)	0.14
Adjusted model 2				
E-IVPD (mm Hg)	0.84 (0.71, 0.97)	0.93 (0.67, 1.19)	0.79 (0.54, 1.04)	0.62
ER-IVPD (mm Hg)	-0.68 (-0.92, -0.45)	-0.99 (-1.41, -0.56)	-1.48 (-1.87, -1.08)	0.009*
A-IVPD (mm Hg)	0.97 (0.84, 1.11)	0.75 (0.50, 1.00)	0.97 (0.72, 1.22)	0.27
S-IVPD (mm Hg)	1.72 (1.49, 1.96)	1.46 (1.03, 1.89)	1.86 (1.39, 2.33)	0.25
SR-IVPD (mm Hg)	-1.17 (-1.34, -0.99)	-0.83 (-1.21, -0.46)	-1.32 (-1.64, -1.01)	0.04†
Adjusted model 3				
E-IVPD (mm Hg)	0.85 (0.72, 0.99)	0.91 (0.63, 1.20)	0.79 (0.54, 1.05)	0.76
ER-IVPD (mm Hg)	-0.72 (-0.96, -0.49)	-0.87 (-1.34, -0.40)	-1.52 (-1.92, -1.13)	0.006*†
A-IVPD (mm Hg)	0.98 (0.85, 1.12)	0.73 (0.46, 1.00)	0.99 (0.73, 1.24)	0.24
S-IVPD (mm Hg)	1.74 (1.5, 1.98)	1.47 (1.01, 1.92)	1.86 (1.37, 2.34)	0.34
SR-IVPD (mm Hg)	-1.17 (-1.35, -0.99)	-0.86 (-1.25, -0.47)	-1.31 (-1.64, -0.99)	0.11

Data are presented as mean (95% CI).

Unadjusted model; adjusted model 1: adjusted for clinical data (age, sex, African American ethnicity, BMI, coronary artery disease, eGFR and beta blocker, ACE-inhibitor, ARB, loop diuretic, and spironolactone use); adjusted model 2: model 1 additionally adjusted for echo parameters (Mitral E-wave velocity, E wave deceleration time, Mitral annular e' septal); adjusted model 3: model 2 additionally adjusted for MRI data (LV mass index and EDVI).

* $p < 0.05$ for No-HF vs HFpEF.

† $p < 0.05$ for HFrEF vs HFpEF.

‡ $p < 0.05$ for No-HF vs HFrEF.

EDVI, end-diastolic volumen index; eGFR, estimated glomerular filtration rate; HF, heart failure; HFpEF, HF with preserved ejection fraction; HFrEF, HF with reduced ejection fraction; IVPD, intraventricular pressure difference; LV, left ventricular.

Diastolic IVPDs

Unadjusted comparisons demonstrated no significant differences in E-IVPD (No-HF=0.76; HFrEF=0.83; HFpEF=0.83 mm Hg; $p=0.63$) and A-IVPD (No-HF=0.93; HFrEF=0.72; HFpEF=0.92 mm Hg; $p=0.07$) between the groups (table 2 and figure 2). In contrast, ER-IVPD was significantly different between the groups (ANOVA $p=0.01$), consistent with a more pronounced reversal of the early diastolic IVPD in HFpEF (-1.30 mm Hg) compared with the No-HF group (-0.78 mm Hg) and the HFrEF group (-0.75 mm Hg). After adjustment for age, sex, African American ethnicity, BMI, coronary artery disease, eGFR and medication use (adjusted model 1), these differences persisted (No-HF=-0.76; HFrEF=-0.85; HFpEF=-1.35 mm Hg; $p=0.02$). Similarly, these differences were present after

further adjustment for Doppler-echocardiographic parameters (adjusted model 2: No-HF=-0.68; HFrEF=-0.99; HFpEF=-1.48 mm Hg; $p=0.009$) and LV structure (adjusted model 3: No-HF=-0.72; HFrEF=-0.87; HFpEF=-1.52 mm Hg; $p=0.006$).

Systolic IVPDs

In unadjusted analyses (table 2 and figure 2), there were significant differences between groups in S-IVPD (No-HF=1.7; HFrEF=1.41; HFpEF=1.99 mm Hg; $p=0.01$) and SR-IVPD (No-HF=-1.15; HFrEF=-0.90; HFpEF=-1.37 mm Hg; $p=0.04$), with more pronounced IVPDs in the HFpEF group compared with the HFrEF group. Between-group differences in SR-IVPD were also present after adjustment for general clinical

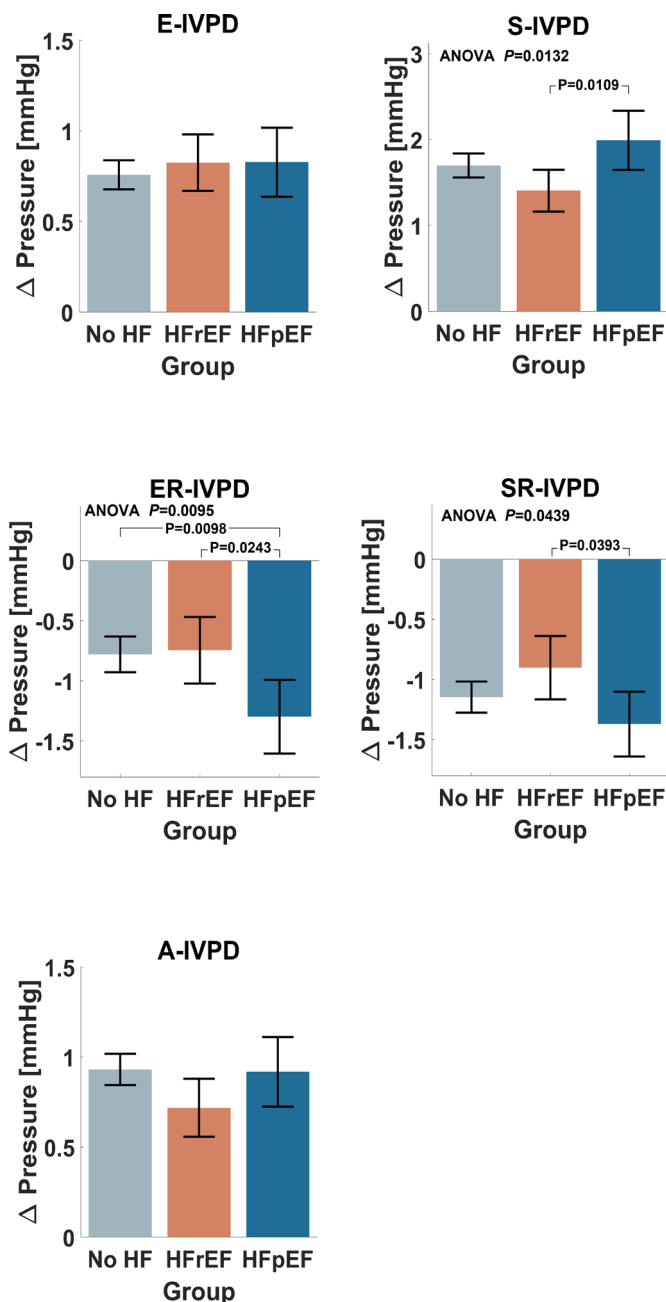


Figure 2 Comparison of IVPDs between groups for the unadjusted model. Computed parameters from diastole (left) and systole (right) are shown. Error bars represent 95% CIs. ANOVA, analysis of variance; HF, heart failure; HFReEF, HF with reduced ejection fraction; HFpEF, HF with preserved ejection fraction; IVPD, intraventricular pressure difference.

characteristics and Doppler-echocardiographic parameters (adjusted model 2; [table 2](#) and [figure 3](#)), but no significant differences in systolic IVPDs were found between the groups after further adjustment for LV structure (adjusted model 3; [table 2](#) and [figure 3](#)).

Reproducibility and repeatability assessment

Higher reproducibility was demonstrated for diastolic E-IVPD and ER-IVPD parameters ($r^2 \geq 0.70$; $SSE \leq 0.58$; $RPC \leq 0.55$) in comparison with A-IVPD ($r^2 = 0.56$;

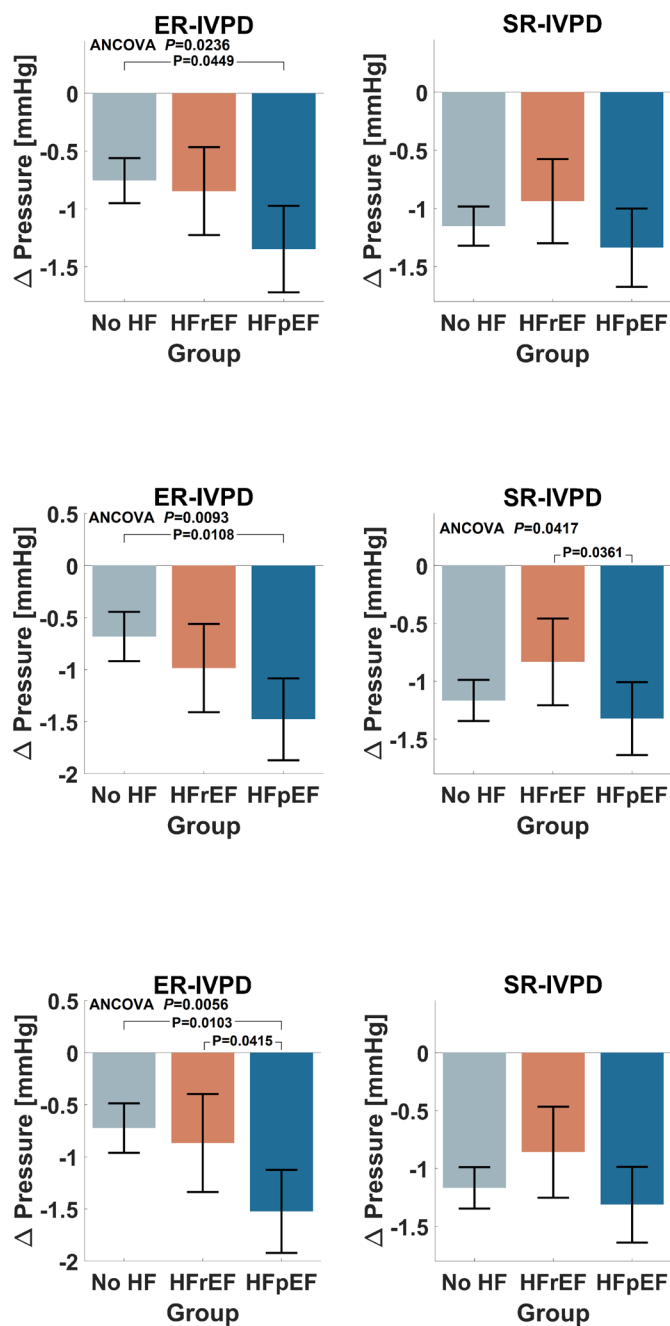


Figure 3 Selected IVPD parameters (ER and SR—wave peak pressures) with statistically significant differences between groups for adjusted models: (top) adjusted model 1; (middle) adjusted model 2; (bottom) adjusted model 3. Computed parameters from diastole (left) and systole (right) are shown. Error bars represent 95% CIs. ANCOVA, analysis of covariance. HF, heart failure; HFReEF, HF with reduced ejection fraction; HFpEF, HF with preserved ejection fraction; IVPD, intraventricular pressure difference.

$SSE = 0.98$; $RPC = 0.65$) and systolic parameters (S-IVPD: $r^2 = 0.04$; $SSE = 5.3$; $RPC = 1.6$; SR-IVPD: $r^2 = 0.47$; $SSE = 1.3$; $RPC = 0.76$). This trend was maintained for the repeatability assessment, although altogether higher indexes were found in this case (diastolic parameters: $r^2 \geq 0.92$; $SSE \leq 0.21$; $RPC \leq 0.32$; systolic parameters: $r^2 \geq 0.71$; $SSE \leq 1.6$; $RPC \leq 0.87$).

Parameter Correlation

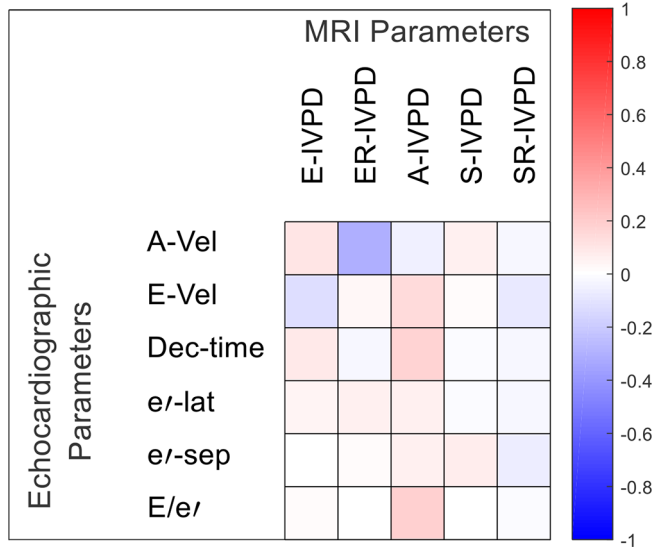


Figure 4 Correlation coefficients between echocardiographic and MRI-based IVPDs parameters, showing correlation between IVPD (MRI-based) parameters: E-wave pressure peak (E-IVPD), E-wave reversal pressure peak (ER-IVPD), A-wave pressure peak (A-IVPD), S-wave pressure peak (S-IVPD) and S-wave reversal pressure peak (SR-IVPD); and echocardiographic parameters: peak E-wave and A-wave velocities by Doppler (E and A-Vel), deceleration time (Dec-time), e' velocity (lateral (e'-lat) and septal (e'-sep)) and E/e'. IVPD, intraventricular pressure difference.

Echocardiographic/MRI correlation assessment

There were only weak correlations between standard Doppler-echocardiographic parameters and IVPD parameters ($R < 0.20$ for all, except for the correlation between ER-IVPD and peak A-wave velocity ($R = -0.30$)). Correlation coefficients between standard Doppler-echocardiographic indices of diastolic function and IVPD parameters are presented in [figure 4](#).

DISCUSSION

We compared diastolic and systolic IVPDs between subjects with HFrEF, HFpEF or No-HF. We found physiologically expected patterns of IVPD in all three groups, with significant differences in diastolic IVPDs. Specifically, subjects with HFpEF exhibited more pronounced reversal peak of early diastolic IVPDs, which was independent of clinical parameters, echocardiographic parameters of LV filling, and LV structure assessed by MRI. Subjects with HFrEF demonstrated a non-significant trend of increasing E-IVPD and decreasing A-IVPD, S-IVPD and SR-IVPD. Our findings suggest distinct patterns of systolic and diastolic IVPDs and differences in the nature of both diastolic and systolic dysfunction between HF subtypes. IVPD parameters demonstrated only weak correlations with standard Doppler-echocardiographic parameters.

Previous studies have shown that, despite being small in magnitude, IVPDs have a significant role in efficient filling and emptying of the LV and could be used

to characterise cardiac performance.^{8 20} However, the assessment and interpretation of intraventricular pressure gradients in clinical practice remains complicated by its dependency on a large number of factors and interactions.^{10 21} Furthermore, flow occurs in multiple and rapidly changing directions, forming complex vortex patterns.^{10 20} The complexity of intraventricular flow and technical limitations of ultrasound imaging, the standard method in cardiovascular assessment, make it difficult to relate intraventricular flow patterns and derived IVPDs to LV myocardial function in a quantitative manner.^{10 20 21}

The increasing availability of cardiovascular MRI has made it an advantageous alternative from a technical point of view due to its high image quality, reproducibility, repeatability, plane of view flexibility, sufficient spatial and temporal resolution and reduced operator dependency. Furthermore, MRI-based IVPD calculations allow for a more flexible definition and alignment of the operator's 'scan line', which could be relevant when the blood flow exhibits a curved trajectory.¹⁷ Additionally, two-dimensional-velocity information from phase contrast MRI improves the accuracy of IVPDs even if the temporal resolution, a critical parameter to calculate IVPDs,²² is lower in comparison with ultrasound. In fact, Thompson and McVeigh¹³ reported that a minimum temporal resolution of 44 ms may avoid significant underestimation of the local acceleration contribution to the total intracardiac pressure differences. Previously, making use of computational fluid dynamics simulations, we assessed the impact of temporal resolution in IVPD calculations, showing that the temporal resolution of phase contrast MRI is, at least in theory, sufficient to resolve IVPDs. Furthermore, we also showed that IVPDs estimated by a one-dimensional method as colour-Doppler ultrasound are larger in magnitude than when the two-dimensional velocity information was used, but the estimates based on two-dimensional velocity information are more accurate, especially in extreme scan line misalignments,²³ which could be particularly sensible after mid and late diastole due to formation of vortices.^{8 14} We speculate that this explains, at least partly, some of the difference between values reported here and in other studies.^{9 15-17}

There were no significant differences in E-IVPD and A-IVPD between the groups. This may be a consequence of early filling pseudonormalisation due to greater filling pressures. Additionally, in HFpEF patients, pronounced diastolic abnormalities can often be elicited only during physiological perturbations, such as exercise or dobutamine infusions,²⁴⁻²⁶ as subjects with HFpEF exhaust their reserve to preserve the diastolic suction force at rest, limiting their ability for adaptation to stress.^{24 25} Nonetheless, our results demonstrate that HFpEF is associated with a greater magnitude of the ER-IVPD. Although, the slope of mitral inflow deceleration temporally coincides with ER-IVPD, it is interesting to note that we did not find significant differences in the deceleration time between the groups, and that ER-IVPD was not strongly related to the deceleration time.

Therefore, our data suggests that ER-IVPD may be a more sensitive marker of diastolic function in HFpEF.

We also examined systolic IVPDs. A typical biphasic IVPD pattern was observed in systole, with a positive peak immediately followed by a negative one. HFrEF individuals exhibited lower values, whereas the HFpEF group presented an overall higher total magnitude of S-IVPD and SR-IVPD, suggesting differences in systolic flow dynamics between groups. These differences could be related to the unsteady nature of ejective flow, abnormalities in chamber geometry, and/or the sequence of regional contraction.²⁰

Our reproducibility and repeatability assessments suggest a general adequate inter and intra-operator variability for early diastolic IVPD parameters. Reproducibility and repeatability were lower for A-IVPD, probably due to a more complex flow after mid and late diastole.^{8,14} Systolic parameters evidenced a need to refine the standardisation of the method, particularly for S-IVPD. The overall correlation between IVPD parameters and echocardiographic indexes was weak or non-existent. In fact, previous publications have pointed out a weak correlation between Doppler echocardiographic estimates of LV filling pressure with invasive filling pressure measurements and the necessity to include further analysis of non-invasive measures.^{27,28} In contrast, echocardiographic^{16,17} and MRI¹³ based IVPD parameters have shown good agreement against invasive intraventricular measurements, adding potentially relevant information for cardiovascular assessments.

The reported data should be interpreted considering the strengths and limitations of the study. Strengths of this study are the inclusion of patients with HFrEF and HFpEF, and the assessment of IVPDs with phase-contrast MRI, which overcomes a number of assumptions made with colour M-mode echocardiography and allows for a more consistent interrogation of intraventricular flow. Our study also has limitations. We did not perform invasive catheter-based measures of distensibility which would have been unfeasible in the absence of a clinical indication for LV catheterisation. From a technical point of view, the MRI acquisition requires relative long breath-holds (~20s) and has limited temporal and through plane spatial resolution, while the processing could be affected by the image alignment and assumptions made about the nature of flow from the three chambers view. On computation of the IVPDs, viscous forces are neglected and it is assumed that inflow and outflow is laminar.^{9,17,25} On average, our HFpEF subjects did not have marked left atrial enlargement, suggesting the presence of mild HFpEF. This may have led to underestimations of true underlying differences. Our population was a clinical sample referred for a cardiac MRI study, which may not fully represent population-based trends. Moreover, complementary myocardial mechanic studies could be included to improve the analysis.²⁹

In conclusion, we demonstrated the feasibility to assess IVPDs throughout the cardiac cycle using phase-contrast MRI and compared IVPDs between subjects without HF

and subjects with HFrEF and HFpEF. Our findings suggest distinct patterns of diastolic IVPDs in HFpEF, implying differences in the nature of diastolic dysfunction between the HF subtypes. Further research is warranted to exploit MRI analysis thoroughly to assess the significance of these novel indices regarding risk stratification and response to therapy.

Contributors Design: FL-H, PS and JAC; oversight and funding: PS and JAC; manuscript drafting: FL-H; critical review of the manuscript: all authors; data collection: GO, MRK, KJ, RM, IV and SA; image analyses: ZH, RB, AT and WW.

Funding This study was supported by NIH grants R56HL-124073-01A1 (JAC), R01 HL 121510-01A1 (JAC), 5-R21-AG-043802-02 (JAC) and a VISN-4 research grant from the Department of Veterans Affairs (JAC).

Competing interests JAC has received consulting honoraria from Bristol Myers Squibb, OPKO Healthcare, Sanifit, Akros Pharma, Fukuda-Denshi, Ironwood, Microsoft, Merck, Bayer and Pfizer. He received research grants from National Institutes of Health, American College of Radiology Network, Fukuda Denshi, Bristol Myers Squibb, Microsoft and CVRx Inc. He is named as inventor in a University of Pennsylvania patent application for the use of inorganic nitrates/nitrites for the treatment of Heart Failure and Preserved Ejection Fraction. Other authors have no disclosures.

Patient consent for publication Not required.

Provenance and peer review Not commissioned; internally peer reviewed.

Data availability statement No data are available.

Open access This is an open access article distributed in accordance with the Creative Commons Attribution Non Commercial (CC BY-NC 4.0) license, which permits others to distribute, remix, adapt, build upon this work non-commercially, and license their derivative works on different terms, provided the original work is properly cited, appropriate credit is given, any changes made indicated, and the use is non-commercial. See: <http://creativecommons.org/licenses/by-nc/4.0/>.

ORCID iD

Julio Alonso Chirinos <http://orcid.org/0000-0001-9035-5670>

REFERENCES

- McMurray JJV, Adamopoulos S, Anker SD, *et al.* ESC guidelines for the diagnosis and treatment of acute and chronic heart failure 2012: the task force for the diagnosis and treatment of acute and chronic heart failure 2012 of the European Society of cardiology. developed in collaboration with the heart failure association (HFA) of the ESC. *Eur Heart J* 2012;33:1787–847.
- Little WC, Zile MR. HFpEF: cardiovascular abnormalities not just comorbidities. *Circulation* 2012;5:669–71.
- Borlaug BA, Paulus WJ. Heart failure with preserved ejection fraction: pathophysiology, diagnosis, and treatment. *Eur Heart J* 2011;32:670–9.
- Ponikowski P, Voors AA, Anker SD, *et al.* 2016 ESC guidelines for the diagnosis and treatment of acute and chronic heart failure. *Eur Heart J* 2016;37:2129–30.
- Nagueh SF, Smiseth OA, Appleton CP, *et al.* Recommendations for the Evaluation of Left Ventricular Diastolic Function by Echocardiography: An Update from the American Society of Echocardiography and the European Association of Cardiovascular Imaging. *J Am Soc Echocardiogr* 2016;29:277–314.
- Oh JK, Park S-J, Nagueh SF. Established and novel clinical applications of diastolic function assessment by echocardiography. *Circ Cardiovasc Imaging* 2011;4:444–55.
- Cameli M, Mondillo S, Solari M, *et al.* Echocardiographic assessment of left ventricular systolic function: from ejection fraction to torsion. *Heart Fail Rev* 2016;21:77–94.
- Greenberg NL, Vandervoort PM, Firstenberg MS, *et al.* Estimation of diastolic intraventricular pressure gradients by Doppler M-mode echocardiography. *Am J Physiol Heart Circ Physiol* 2001;280:H2507–15.
- Greenberg NL, Vandervoort PM, Thomas JD. Instantaneous diastolic transmitral pressure differences from color Doppler M mode echocardiography. *Am J Physiol Heart Circ Physiol* 1996;271:H1267–76.
- Nagueh SF, Appleton CP, Gillebert TC, *et al.* Recommendations for the evaluation of left ventricular diastolic function by echocardiography. *Eur J Echocardiogr* 2009;10:165–93.

- 11 Paulus WJ, Tschöpe C, Sanderson JE, *et al.* How to diagnose diastolic heart failure: a consensus statement on the diagnosis of heart failure with normal left ventricular ejection fraction by the heart failure and echocardiography associations of the European Society of cardiology. *Eur Heart J* 2007;28:2539–50.
- 12 Chirinos JA, Akers SR, Trieu L, *et al.* Heart failure, left ventricular remodeling, and circulating nitric oxide metabolites. *J Am Heart Assoc* 2016;5.
- 13 Thompson RB, McVeigh ER. Fast measurement of intracardiac pressure differences with 2D breath-hold phase-contrast MRI. *Magn Reson Med* 2003;49:1056–66.
- 14 Steine K, Stugaard M, Smiseth OA. Mechanisms of diastolic intraventricular regional pressure differences and flow in the inflow and outflow tracts. *J Am Coll Cardiol* 2002;40:983–90.
- 15 Firstenberg MS, Vandervoort PM, Greenberg NL, *et al.* Noninvasive estimation of transmitral pressure drop across the normal mitral valve in humans: importance of convective and inertial forces during left ventricular filling. *J Am Coll Cardiol* 2000;36:1942–9.
- 16 Yotti R, Bermejo J, Antoranz JC, *et al.* A noninvasive method for assessing impaired diastolic suction in patients with dilated cardiomyopathy. *Circulation* 2005;112:2921–9.
- 17 Yotti R, Bermejo J, Desco MM, *et al.* Doppler-derived ejection intraventricular pressure gradients provide a reliable assessment of left ventricular systolic chamber function. *Circulation* 2005;112:1771–9.
- 18 Ebbers T, Wigström L, Bolger AF, *et al.* Estimation of relative cardiovascular pressures using time-resolved three-dimensional phase contrast MRI. *Magn. Reson. Med.* 2001;45:872–9.
- 19 Buyens F, Jolivet O, De Cesare A, *et al.* Calculation of left ventricle relative pressure distribution in MRI using acceleration data. *Magn. Reson. Med.* 2005;53:877–84.
- 20 Yotti R, Bermejo J, Antoranz JC, *et al.* Noninvasive assessment of ejection intraventricular pressure gradients. *J Am Coll Cardiol* 2004;43:1654–62.
- 21 Pasipoularides A. Right and left ventricular diastolic flow field: why are measured intraventricular pressure gradients small? *Revista espanola de cardiologia* 2013;66:337–41.
- 22 Rojo-Álvarez JL, Bermejo J, Rodríguez-González AB, *et al.* Impact of image spatial, temporal, and velocity resolutions on cardiovascular indices derived from color-Doppler echocardiography. *Med Image Anal* 2007;11:513–25.
- 23 Londono-Hoyos FJ, Swillens A, Van Cauwenberge J, *et al.* Assessment of methodologies to calculate intraventricular pressure differences in computational models and patients. *Med Biol Eng Comput* 2018;56:469–81.
- 24 Ohara T, Niebel CL, Stewart KC, *et al.* Loss of adrenergic augmentation of diastolic intra-LV pressure difference in patients with diastolic dysfunction: evaluation by color M-mode echocardiography. *JACC Cardiovasc Imaging* 2012;5:861–70.
- 25 Rovner A, Greenberg NL, Thomas JD, *et al.* Relationship of diastolic intraventricular pressure gradients and aerobic capacity in patients with diastolic heart failure. *Am J Physiol Heart Circ Physiol* 2005;289:H2081–8.
- 26 Gillebert TC, HFpEF DBML. Diastolic suction, and exercise. *JACC Cardiovasc Imaging* 2012;5:871–3.
- 27 Mitter SS, Shah SJ, Thomas JD. A test in context: E/A and E/e' to assess diastolic dysfunction and LV filling pressure. *J Am Coll Cardiol* 2017;69:1451–64.
- 28 Park J-H, Marwick TH. Use and limitations of E/e' to assess left ventricular filling pressure by echocardiography. *J Cardiovasc Ultrasound* 2011;19:169–73.
- 29 Edvardsen T, Rosen BD, Pan L, *et al.* Regional diastolic dysfunction in individuals with left ventricular hypertrophy measured by tagged magnetic resonance imaging—The multi-ethnic study of atherosclerosis (MESA). *Am Heart J* 2006;151:109–14.